OMICS Journal of Radiology
ISSN: 2167-7964

Förschler et al., OMICS J Radiol 2016, 5:4
DOI: 10.4172/2167-7964.1000232

Research Article Open Access

Brain Tumor Heterogeneity: Voxel-wise Correlational Study of MR Perfusion and 2D MR Spectroscopic Imaging

Annette Förschler[1*], Katharina Schwede[2], Mirjam Ines Schubert[3], Claus Zimmer[3] and Dirk Winkler[4]

[1]*Institute of Clinical and Interventional Neuroradiology, Vivantes Klinikum Neukölln, Berlin, Germany*

[2]*Department of Dermatology, Venereology and Allergology, University Hospital, University of Leipzig, Leipzig, Germany*

[3]*Department of Neuroradiology, Klinikum rechts der Isar, Technical University Munich, Munich, Germany*

[4]*Department of Neurosurgery, University Hospital, University of Leipzig, Leipzig, Germany*

[*]**Corresponding author:** Annette Förschler, Institute of Clinical and Interventional Neuroradiology, Vivantes Klinikum Neukölln, Rudower Str. 48, 12351 Berlin, Germany, Tel: +49-163-3450501; Fax: +49-30-35504776; E-mail: annette.foerschler@gmx.de

Received date: June 22, 2016; **Accepted date:** August 16, 2016; **Published date:** August 19, 2016

Copyright: © 2016 Förschler A, et al. This is an open-access article distributed under the terms of the Creative Commons Attribution License, which permits unrestricted use, distribution, and reproduction in any medium, provided the original author and source are credited.

Abstract

An accurate characterization of glioma heterogeneity is essential when determining tumor grade and the most appropriate therapy target. Non-invasive imaging modalities such as MR perfusion imaging (PWI) and 2D proton MR spectroscopic imaging (MRSI) can provide functional and metabolic information about the tumor to assist in this task. Using a voxel-wise correlation we aimed at investigating whether both MRSI and PWI characterize brain tumor heterogeneity similarly, and, whether the regions of their most pathologic values coincide.

In 31 patients with different primary brain tumors rCBV and rCBF were correlated to the metabolites Cho, Cr and NAA and the metabolite ratios Cho/Cr, NAA/Cr and Cho/NAA on a voxel-wise basis. Intraindividually, we tested for significant relationships and we recorded the reliability and the direction of these relationships by calculating the inter individual variance of Kendall's correlation coefficient τb. Additionally, the locations of the most pathologic values of PWI and MRSI were compared. Across all tumors we found no reliable relationship between perfusion and spectroscopic measures apart from a positive correlation of rCBV and rCBF with Cr, mainly based on a positive correlation in II° gliomas and glioblastomas but not in III° gliomas or lymphomas. The separate analysis of the tumor groups revealed consistent correlations of additional value pairs in II° gliomas and glioblastomas, but not in III° gliomas or lymphomas. The overall spatial concordance rate between the maximum perfusion values and the most pathological metabolite values was 34%. Our results suggest that brain tumors display heterogenous correlation pattern of the perfusion markers of malignancy to the spectroscopy-derived malignancy markers. As the single modality methods may display different kinds of tumor hot spots, PWI and MRSI should be fused to allow for more specific therapy planning of brain tumors.

Keywords: Brain Tumors; MR Spectroscopy; MR Perfusion Imaging; Brain Tumor Heterogeneity; Neurooncology

Abbreviations:

CBF: Cerebral Blood Flow; CBV: Cerebral Blood Volume; Cho: Choline; Cr: Creatine; MR: Magnetic Resonance; MRS: Proton Magnetic Resonance Spectroscopy; MRSI: Multi-Voxel Proton MR Spectroscopic Imaging; NAA: N-acetylaspartate; PWI: Perfusion Weighted Imaging; rCBV: Relative Cerebral Blood Volume; rCBF: Relative Cerebral Blood Flow; TE: Echo Time; TR: Repetition Time; VOI: Volume of Interest; WHO: World Health Organization

Introduction

In contrast to the mostly homogeneous primary central nervous system lymphomas, gliomas, especially those of higher grades, are known to be heterogeneous. In a single tumor, areas of different malignancy can occur [1]. This fact is of particular interest in various contexts. It is crucial to detect the most malignant part of the whole lesion because the prognosis of the patient and the therapy regimen among other things depend upon the tumor grade [2]. The WHO Grading system [3] lists mitotic activity, cell density and vessel proliferation – among others – as histological criteria for anaplastic transformation. However, conventional magnetic resonance (MR) imaging is limited in depicting these different biological behaviors.

Dynamic susceptibility weighted contrast enhanced MR perfusion weighted imaging (PWI) assists in the differential diagnosis, grading and/or therapy planning of neoplastic brain lesions. The perfusion parameters cerebral blood volume (CBV) and cerebral blood flow (CBF) are of special interest. The CBV is linked to the microvessel density [4] and has proven to be superior regarding glioma grading [5], but the CBF also increases along with malignancy [6].

Proton MR spectroscopy (MRS) is a non-invasive, MR-based tool which may indirectly provide additional pathophysiological and metabolic information: The MRS-derived metabolite choline (Cho), indicating cell density and proliferation, is known to be elevated in brain tumors and to increase with the degree of malignancy [7]. On the other hand, N-acetylaspartate (NAA), representing neuronal density and viability, decreases in most pathological states including brain neoplasms [8]. The metabolite total creatine (creatine plus phosphocreatine; Cr) is widely used as an internal reference [9]. Interestingly, Cr has also been shown to rise in gliomas, which was associated with a tendency to earlier tumor progression [10,11]. In contrast to single voxel MRS, two-dimensional multi-voxel proton MR

spectroscopic imaging (MRSI), provides the opportunity to acquire multiple spectra, and, hence, to visualize the spatial distribution of the metabolite levels [12].

PWI and MRSI were used earlier in order to monitor and to predict malignant transformation of gliomas. Hlaihel et al. [13] reported that MRSI was able to detect the malignant glioma transformation earlier than PWI, whereas Weber et al. [14] showed that PWI was more sensitive in the early detection of anaplastic transformation. Of note, both PWI and MRSI displayed pathological measures in the same tumor location. However, previous studies suggested that this was not necessarily the case. Wagner et al. [15] found spatial divergence between the areas of the highest rate of neovascularisation–represented by CBV–and the areas of tumor cell proliferation–imaged by Cho. Some of these studies dealed with only the maximal values, others investigated just selected perfusion parameters or metabolites. In contrast, the aim of our study was to comprehensively evaluate whether the perfusion markers of malignancy corresponded to the spectroscopy-derived malignancy markers. For this, we correlated – on a voxel-wise basis – the CBV and CBF to the spectroscopically derived metabolites NAA, Cho and Cr and their ratios NAA/Cr, Cho/Cr and Cho/NAA, respectively. In addition, we explored whether or not there was a spatial correlation between the maximum PWI and most pathological MRSI parameters investigated.

Materials and Methods

This study was approved by the local ethics committee. Patients with known or suspected primary brain tumors preoperatively underwent MR imaging including MRSI and PWI. Inclusion criteria for the study were histological diagnosis of primary brain tumor (as revealed by open surgery or stereotactic biopsy) and written informed consent. Only MR images with no or only minor artifacts on all MR-sequences were accepted for further analysis.

Thirty-one patients (19 male, 12 female, mean age 58 years, range 18–76 years) met the inclusion criteria. According to neuropathology, patients were subdivided into the following groups: II° glioma (n=5), III° glioma (n=7), glioblastoma (n=12), and primary cerebral lymphoma (n=7). The MR examinations were performed on a 1.5 T whole body scanner (MAGNETOM® Symphony; Siemens AG, Erlangen, Germany) equipped with a phased array head coil. Axial and coronal T2-weighted images were acquired to facilitate positioning of the MRS voxels. 2D-MRSI (2D PRESS, repetition time (TR)/echo time (TE)=1500/135 ms, matrix=16^2, FOV=160 × 160 mm^2, slice thickness = 10 mm) resulted in spectroscopic voxels measuring 1 cm^3. Outer volume suppression led to a volume of interest (VOI) which was 8 × 8 × 1 cm^3 in size and was adjusted to contain tumor tissue and contralateral healthy tissue, avoiding lipid bearing skull structures. The spectroscopic data were acquired prior to the application of contrast media to avoid any potential contrast-induced alterations, in particular, with regards to the choline peak height and area [16]. After the axial contrast-enhanced T1-weighted scan PWI was conducted using the contrast agent Gadolinium-diethylenetriamine pentaacetic acid (Gd-DTPA; Magnevist®, Bayer Schering Pharma AG, Berlin, Germany) at a dose of 0.1 mmol/kg, twice. The first (weight-adjusted) amount of contrast agent was given at a flow rate of 1.5 mL/s followed by a 20 mL bolus of 0.9% saline. This resulted in contrast agent presaturation of the extravascular space in tumor areas with disrupted blood brain barrier, minimizing the underestimation of the CBV due to contrast extravasation. The second bolus of Gd-DTPA was started simultaneously with the PWI measurement at a flow rate of 5 mL/s flushed with 20 mL of saline.

For the perfusion measurements, a total of 20 slices were acquired with 25 repeated images for each slice (spin-echo EPI, TR/TE = 2000/60 ms, matrix = 128^2, slice thickness = 3 mm without slice gap). The FOV (256 × 256 mm^2), the number and the position of the slices were identical to the T2 and T1 weighted axial sequences. All data were processed with the Software Syngo® (Siemens Healthcare, Erlangen, Germany). Color coded maps of CBF and CBV were calculated using the "Neuro Perfusion Evaluation" tool. The parameters CBF and CBV were estimated by deconvolving the course of tissue signal intensities over the first pass contrast bolus with an arterial input function (AIF) [17,18]. For this, the global AIF was selected manually by averaging a small number of concentration-time curves from voxels in the vicinity of the main insular branches of the middle cerebral artery of the contralateral hemisphere, allowing for the definition of the beginning and the end of the first-pass bolus.

For coregistration, the matrix grid of the MRSI was superimposed onto the color coded CBV and CBF maps as well as onto the axial T2 and contrast enhanced T1 weighted reference slices for anatomical orientation. The borders of each spectroscopic voxel within the tumors were traced manually and were transferred onto the perfusion maps as VOIs (Figure 1).

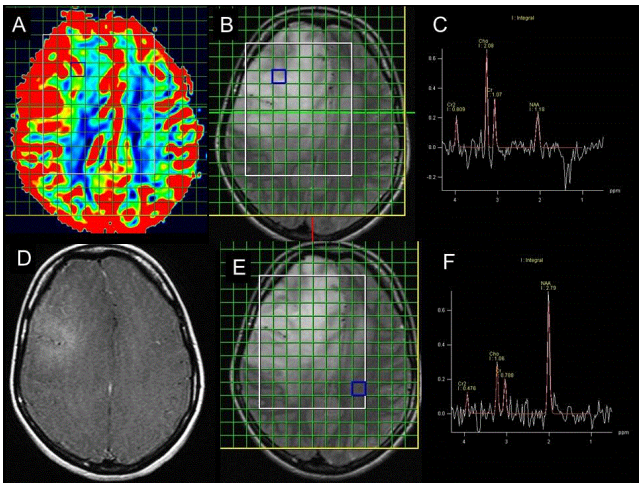

Figure 1: Example of a patient with an anaplastic astrocytoma (WHO III°). Within the right frontal tumor, highly perfused areas (red) are noted on the CBV map (A) and faint contrast enhancement on T1 weighted images (D). The spectroscopy grid element is superimposed on CBV map and on the T2 images (B, E). The spectrum (C) was taken from the blue outlined voxel in (B) within the tumor and displays markedly elevated choline, NAA decrease and a lactate double peak. The spectrum (F) was taken from the blue outlined voxel in (E) within the contralateral hemisphere and displays normal metabolite values.

Thus, for each spectroscopic voxel the corresponding perfusion values were extracted, and, in order to achieve better inter-subject comparability, were normalized to normal appearing white matter (NAWM). This produced the relative (r) perfusion values rCBV and rCBF. Using the Syngo "Spectroscopy Evaluation" tool metabolite peak integrals and their ratios were estimated for each voxel within the

tumor and were referenced to NAWM resulting in rNAA, rCho, rCr, rNAA/Cr, rCho/Cr and rCho/NAA. For reasons of simplification, 'r' indicating relative values is omitted henceforth. Spectra and perfusion maps were carefully evaluated by an experienced neuroradiologist and voxels with noisy or distorted spectra or physiological hyperperfusion (e.g., cortical and deep grey matter) were excluded from further analysis.

For statistical analysis SPSS® Version 11.5 (SPSS Inc., Chicago, Illinois) was used.

In a first step, for every particular tumor a correlation analysis of all included VOIs was performed. Due to the lack of a bivariate normal distribution and linear relationship for each value pair, as well as, due to the small sample size in some individuals the Kendall's rank correlation was applied: By correlating CBV and CBF to each metabolite and metabolite ratio, respectively we collected the Kendall's correlation coefficients τb of each individual patient and determined the corresponding level of significance. τb can range in value from –1 (a perfect negative association, or perfect inversion) to +1 (a perfect positive association, or perfect agreement). A value of 0 indicates no association. Only the intra-individual value pairs with a significant relationship ($p<0.05$) were included in the further analysis.

In a second step, for all 12 pairs of values the inter-individual variances of these τb coefficients were assessed. In a systematic relationship of a value pair the algebraic sign of τb is constant across all patients. On the other hand, a broad variance of (positive and negative) τb identifies random significances.

Additionally, the maximal or most pathologic values of CBV and CBF (CBV_{max}, CBF_{max}, respectively), as well as of the metabolites (Cho_{max}, Cr_{max}, NAA_{min}, Cho/Cr_{max}, Cho/NAA_{max}, NAA/Cr_{min}) were located. Furthermore, for all 12 PWI-MRSI pairs of values, it was examined whether the areas of maximum perfusion values matched or adjoined the spectroscopic voxels displaying the most malignant metabolic tumor profile.

Results

On average, 28 voxels per patient (range 12–60) could be used for evaluation. For reasons of simplicity, the term 'value pair' is used in the following paragraphs representing the association between the quantitative MR perfusion and MRSI measures per voxel within the brain tumor.

Associations between perfusion and metabolite/metabolite ratios in the whole brain tumor cohort

Per value pair, the percentage of patients with significant correlations was relatively small (mean 27%, range 13-39%). However, there were significant correlations in all value combinations (Table 1). Interestingly, we found that more significant correlations emerged from the value pairs of perfusion and metabolite ratios than from the value pairs of perfusion parameters and single metabolites. The highest percentage of patients with significant correlations was found in the value pairs CBV–Cho/NAA and CBF–Cho/NAA, respectively (39%), followed by the value pairs CBV–Cho/Cr and CBV–NAA/Cr (32%). Furthermore, a minor variance of the τb correlation coefficient was observed in the value pairs CBV–Cr and CBF–Cr indicating a systematic relationship. All other value pairs revealed both positive and negative τb with a wide variety, and the respective mean values of τb did not differ much from 0. However, the mean τb in all value pairs pointed in the expected direction, hence the τb of CBV or CBF to NAA or NAA/Cr showed negative means.

n=31	CBV		CBF	
	% significant cases (n=)	τb of significant cases [mean ± SD]	% significant cases (n=)	τb of significant cases [mean ± SD]
Cho	19 (6)	0.28 ± 0.36	23 (7)	0.27 ± 0.33
Cr	13 (4)	0.31 ± 0.06	19 (6)	0.33 ± 0.06
NAA	26 (8)	-0.32 ± 0.29	32 (9)	-0.18 ± 0.36
Cho/Cr	32 (9)	0.19 ± 0.39	19 (6)	0.12 ± 0.47
Cho/NAA	39 (12)	0.30 ± 0.32	39 (12)	0.29 ± 0.32
NAA/Cr	32 (9)	-0.27 ± 0.20	29 (9)	-0.02 ± 0.39

Table 1: Percentage of patients with significant correlations ($p \leq 0.05$) between the MRSI derived metabolites/metabolite ratios and CBV and CBF, respectively, in the brain tumors and the mean value (mean) and standard deviation (SD) of Kendall's τb correlation coefficient (τb b) of the significant associations.

Associations between perfusion and metabolite/metabolite ratios per tumor type

Regarding the different tumor subgroups (Table 2, Figure 2) the highest rate of significant PWI-MRSI correlations was found in II° gliomas (mean 35%, range 20–80%), where the positive association between CBF and Cr (80%) was predominant followed by the positive association between CBV and Cr (60%).

Whenever the number of significant correlations was high enough to allow for an estimation of the mean variation of τb, τb showed only a minor variance (Figure 2A). Of note, although glioblastomas (Figure 2C) revealed the largest number of value pairs with minor variances of τb (all pairs with a computable mean variation except for CBF–NAA, CBV–NAA/Cr and CBF–NAA/Cr) only a relatively low percentage of significant correlations (mean 26%, range 8-50%) emerged. Value pairs without any significant correlations were found in III° gliomas (mean rate of correlations 30%, range 0-57%) and in lymphomas (mean 20%, range 0-57%). These two groups also showed broad dispersion of τb in the value combinations with a high rate of significant correlations (Figures 2B and 2D), which indicates that there was no systematical relationship (in the glioma III group in 57% of the patients the correlations of CBV and Cho/NAA as well as of CBV and NAA/Cr were significant with a τb of 0.21 ± 0.35 and -0.15 ± 0.26, respectively. In lymphomas, CBF and Cho/NAA also correlated in 57%, but with a τb of 0.2 ± 0.42, again, no reliable relationship could be shown).

		glioma II°, n=5		glioma III°, n=7		glioblastoma, n=12		lymphoma, n=7	
		% significant cases (n=)	τb of significant cases [mean ± SD]	% significant cases (n=)	τb of significant cases [mean ± SD]	% significant cases (n=)	τb of significant cases [mean ± SD]	% significant cases (n=)	τb of significant cases [mean ± SD]
CBV	Cho	40 (2)	0.42 ± 0.23	14 (1)	0.33	17 (2)	0,45 ± 0,14	14 (1)	-0.41
	Cr	60 (3)	0.32 ± 0.07	–	–	8 (1)	0.27	–	–
	NAA	20 (1)	-0.27	43 (3)	-0.18 ± 0.48	25 (3)	-0.43 ± 0.08	14 (1)	-0.50
	Cho/Cr	20 (1)	-0.42	43 (3)	0.15 ± 0.32	25 (3)	0.47 ± 0.13	43 (3)	0.14 ± 0.51
	Cho/NAA	20 (1)	0.30	57 (4)	0.21 ± 0.35	33 (4)	0.46 ± 0.20	43 (3)	0.18 ± 0.49
	NAA/Cr	40 (2)	-0.30 ± 0.07	57 (4)	-0.15 ± 0.26	33 (4)	-0.38 ± 0.12	–	–
CB F	Cho	40 (2)	0.44 ± 0.22	14 (1)	0.34	25 (3)	0.37 ± 0.16	14 (1)	-0.44
	Cr	80 (4)	0.35 ± 0.07	14 (1)	0.28	8 (1)	0.30	–	–
	NAA	20 (1)	-0.31	43 (3)	-0.13 ± 0.44	33 (4)	-0.23 ± 0.36	29 (2)	-0.10 ± 0.56
	Cho/Cr	20 (1)	-0.49	14 (1)	0.36	17 (2)	0.45 ± 0.17	29 (2)	-0.02 ± 0.64
	Cho/NAA	40 (2)	0.37 ± 0.05	29 (2)	0.05 ± 0.46	33 (4)	0.46 ± 0.20	57 (4)	0.20 ± 0.42
	NAA/Cr	20 (1)	-0.41	29 (2)	-0.00±0.39	50 (6)	0.04±0.43	–	–

Table 2: Percentage of patients with significant correlations ($p \leq 0.05$) between the MRSI derived metabolites/metabolite ratios and CBV and CBF, respectively, in the different brain tumor groups and the mean value (mean) and standard deviation (SD) of Kendall's tau b correlation coefficient (τb b) of the significant associations.

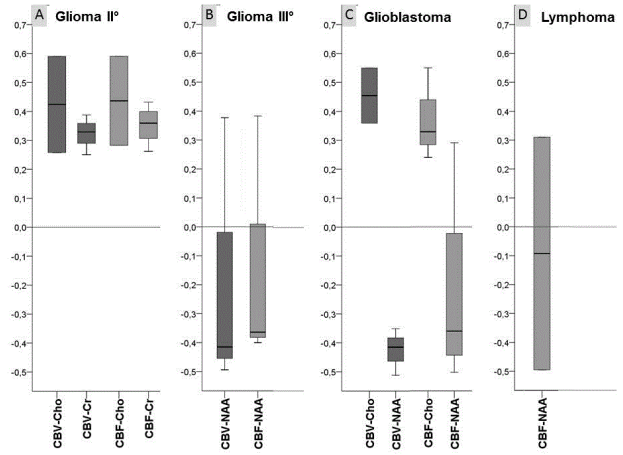

Figure 2: Significant correlations of MRSI-derived metabolites and perfusion parameters (CBV, CBF) subdivided by tumor type and indicated by Kendall's τb mean value and variance. The box plots show the variances of the Kendall's τb correlation coefficient (τb) for all CBV-metabolite (dark gray) and CBF-metabolite (light gray) value pairs with more than one significant correlation. The highest rate of significant PWI-MRSI correlations was found in II° gliomas (A). Significant PWI-MRSI correlations of Glioblastomas are shown in (C). Value pairs without any significant correlations were found in III° gliomas (B) and in lymphomas (D).

Spatial concordance between maximum perfusion parameters and most pathological metabolite/metabolite ratios per tumor type

Overall, the maximal values of the MR perfusion-derived CBV / CBF and the MRSI derived metabolites / metabolite ratios matched or neighbored each other in 34% of the cases (Table 3). Among these, the highest rate of concordance was observed in Cho/NAA_{max} with CBV_{max} (39%) and CBF_{max} (42%), respectively, but also in CBF_{max} and NAA_{min} (39%).The highest overall matching and neighbouring rate occurred (mean: 46%, range 14-71%) in gliomas III°; thereby, the highest rate of concordance was observed in CBF_{max} to NAA_{min} (71%) and CBF_{max} to Cho/NAA_{max} (71%). Glioblastomas displayed a spatial concordance of maximum perfusion parameters and most pathological metabolites/metabolite ratios of 35% (17-50%), with the highest rate of concordance between CBF_{max} and Cho_{max}, Cho/Cr_{max} and NAA_{min}, respectively (50% each pair). In low grade gliomas (mean 30%, range 0-80%) most frequently CBF_{max} and Cr_{max} coincided (80%) followed by the concordance between CBV_{max} and Cr_{max} (60%) and Cho_{max} (60%), respectively. This corresponds to the good correlation between Cr and CBF and CBV, respectively, that we found in the voxel-wise analysis. Of note, no concordance emerged from CBV_{max} or CBF_{max} and NAA_{min} or NAA/Cr_{min}. Interestingly, lymphomas exhibited the lowest rates of maximum value pair concordance (mean 21%, range 0% to 43%) with the highest percentage of concordance in CBV_{max}–Cho/NAA_{max} (43%) and CBF_{max}–Cho/NAA_{max} (43%).

% matching or neighboring (n=)		glioma II	glioma III	glioblastoma	lymphoma	all tumors
		n = 5	n = 7	n = 12	n = 7	n = 31
CBV_{max}	Cho_{max}	60 (3)	14 (1)	42 (5)	14 (1)	32 (10)
	Cr_{max}	60 (3)	29 (2)	17 (2)	14 (1)	26 (8)
	NAA_{min}	–	57 (4)	42 (5)	29 (2)	35 (11)
	Cho/Cr_{max}	20 (1)	57 (4)	42 (5)	14 (1)	35 (11)
	Cho/NAA_{max}	40 (2)	57 (4)	25 (3)	43 (3)	39 (12)
	NAA/Cr_{min}	–	57 (4)	42 (5)	29 (2)	35 (11)
CBF_{max}	Cho_{max}	40 (2)	14 (1)	50 (6)	29 (2)	35 (11)
	Cr_{max}	80 (4)	29 (2)	17 (2)	14 (1)	29 (9)
	NAA_{min}	–	71 (5)	50 (6)	14 (1)	39 (12)
	Cho/Cr_{max}	20 (1)	43 (3)	50 (6)	–	32 (10)
	Cho/NAA_{max}	40 (2)	71 (5)	25 (3)	43 (3)	42 (13)
	NAA/Cr_{min}	–	57 (4)	25 (3)	14 (1)	26 (8)
mean		30 (1,5)	46 (3,3)	35 (4,3)	21 (1,5)	34 (10,5)

Table 3: Percentage of spatial concordance of maximum perfusion values and most pathological metabolite values within the brain tumors.

Discussion

Brain tumors do not necessarily display the most malignant spectra and the highest perfusion values in the same location at the same time [15]. By a voxel-wise correlational and spatial concordance analysis of altered perfusion and metabolism in brain tumors, this study aimed at defining whether the metabolic properties of heterogeneous tumors were correlated with the perfusion distribution.

The main findings of the voxel-wise correlational investigation were an overall positive correlation of Cr to CBV and CBF, respectively, mainly based on a positive correlation of Cr to CBV and CBF, respectively, in II° gliomas and glioblastomas but not in III° gliomas or lymphomas. However, tumor group-wise analysis also revealed that in the other value pairs there was a consistence of the correlations in II° gliomas and, although few in number, in glioblastomas as well. Lymphomas and III° gliomas displayed no such consistent correlation. The spatial concordance analysis, on the other hand, revealed an overall spatial concordance rate between the maximum perfusion values and the most pathological metabolite and metabolite ratio values in approximately one third of the patients only, suggesting that cellular proliferation may not necessarily be linked to vascular proliferation in brain tumors (and vice versa).

Several studies have suggested that proton spectroscopy may be a helpful tool in glioma grading and, hence, in depicting malignant areas within the tumor. However, sensitivity and specificity varied to a large degree among the studies, and it remains unclear which metabolite is the most sensitive and specific [19]. The Cho/Cr ratio has demonstrated the value of Cho in glioma grading [20]. Although the Cho/NAA ratio was also found to be a good marker for locating lesions with high cellular proliferation [11] and for differentiation of irradiation necrosis and tumor recurrence [21], elevated Cho/NAA ratios were reported to persist in necrotic regions [22]. In the present study, the spatial fusion of morphologic, perfusion and spectroscopic imaging allowed for the identification of necrotic tissue, and, hence, its primary exclusion from further analysis.

According to our analysis, Cho correlated reliably with CBV but also with CBF in II° gliomas and in glioblastoma. This is in line with the findings of Catalaa et al. who reported a correlation of mean Cho and mean CBV in the glioblastomas of 21 patients [23]. Using single voxel spectroscopy, Toyooka et al. showed that Cho correlated with CBV [24]. By picking the areas of maximal and minimal CBV, the Cho/Cr ratio was reported to also correlate well with CBV in non-enhancing WHO II° and III° tumors [25]. In our cohort, the Cho/Cr ratio and CBV reliably correlated in glioblastomas when taking into account all tumor areas only.

Interestingly, we found an overall positive correlation between Cr and both perfusion parameters (CBV and CBF). The spectroscopically-derived metabolite creatine represents the total entity of phosphorylated and unphosphorylated tissue creatine, and is predominantly involved in energy pathways and intracellular metabolism. Although Cr is thought to be stable in a broad variety of diseases [12], varying Cr levels in brain tumors were observed previously [9,10]: Cr can be found decreased in brain tumors [26]. Cr has also been shown to rise in gliomas. Interestingly, this was associated with a tendency towards earlier tumor progression [10]. The mechanism of Cr elevation has not yet been fully understood and it has been hypothesized to be caused by either glia activation due to tumor infiltration [10,27] or an inflammatory reaction related to malignant proliferation [28]. Our observations of Cr positively correlating with CBV and CBF lead us to suggest that there may be either different stages of energy demands (anaerobic vs. aerobic metabolism), vascularization with increasing malignancy or different underlying pathophysiology/pathological behavior. Of note, Guillevan et al. reported a significant correlation of CBV_{max} and the single voxel

spectroscopy-derived metabolic ratios lactate/Cr, Cho/NAA, and free-lipids/Cr but not in Cr, and proposed the Lac/Cr ratio to predict regional hemodynamic changes in II° gliomas [13]. Interestingly, in our data together with the results from the voxel-wise correlational study, II° gliomas exhibited a very high spatial concordance rate of CBF_{max} and Cr_{max} followed by the high concordance rate between CBV_{max} and Cr_{max}, respectively.

In our study, low grade gliomas and, to a lesser extent, glioblastomas exhibited a significant positive association between Cr and both perfusion parameters, whereas the tumor group-wise analysis revealed no reliable correlation in III° gliomas and lymphomas. The correlation of CBV and CBF with Cr in II° glioma is remarkable: Low grade gliomas by definition do not display neovascularization, apart from oligodendrogliomas who have a high Cr and more vessels compared to astrocytomas. In our cohort of the 5 glioma II° only one was an oligoastrocytoma. But 4 out of 5 Patients showed the same good corellation of CBF and Cr. Therefore the correlation may be due to the fact that brain tissue with less tumor infiltration may hold a better perfusion along with less deprived Cr. Of note, similar Cr levels were found in both non-enhancing and enhancing III° gliomas [29]. This indicates that Cr levels are independent from the quality of vasculature in III° gliomas. On the other hand, III° glioma is considered as an intermediate stage in a progressive malignant transformation from II° glioma to glioblastoma. Sugahara et al. reported different spatial distributions of areas of blood brain barrier breakdown and elevated CBV levels in anaplastic astrocytomas [4]. Hlaihel et al. observed that in the case of malignant transformation from low to high grade glioma, the elevation of the Cho/Cr level preceded the CBV increase by 12 months [13]. Both circumstances can lead to a transient lack of correlation of perfusion and spectroscopic values as was found in our study. Additionally, in a rat model of malignant glioma, Thorsen et al. observed two tumor phenotypes which developed one after the other, i.e., increased Cho and decreased NAA in the first one was characterized by an intact blood-brain barrier, lack of infiltrative growth and a high amount of stem cells compared to the serially arising one which was characterized by neoangiogenesis and necrosis, thus proposing a higher degree of malignancy [30]. Interestingly, in the spatial concordance analysis, III° gliomas displayed the highest rate of concordance, in particular between CBF_{max} to NAA_{min} and CBF_{max} to Cho/NAA_{max}. This may represent focal hot spots of malignancy.

The vessel density and perfusion of lymphomas is significantly lower compared to high grade gliomas and also slightly lower than in low grade gliomas [31]. In contrast, spectroscopy revealed similar metabolic patterns, i.e., Cho/Cr, Cho/NAA and NAA/Cr ratios, in lymphomas and high grade gliomas [32]. This indicates a lack of coupling between cellular proliferation and angiogenesis in lymphomas compared to gliomas, a finding which was supported by our results for lymphomas which displayed no consistent voxel-wise correlation and the lowest rate of spatial concordance.

Overall, only one third of our patients demonstrated spatial concordance between the maximum PWI-derived CBV or CBF and spectroscopy-derived metabolites. On the other hand, the lack of spatial concordance between perfusion and metabolic information within brain tumors, in particular in anaplastic astrocytomas and glioblastomas (as well as lymphomas) as seen in our study, may be explained by the finding that tumor neovascularization does not necessarily lead to a higher CBV or CBF either due to tumor vessel thrombosis [33] and/or due to vessel compression induced by elevated tissue pressure caused by endothelial leakage in the presence of disrupted blood brain barrier [34]. Furthermore, high grade gliomas in particular are known to be very inhomogeneous with areas of vascular proliferation along with areas of necrosis due to hypoxia [35]. Similarly, histological studies of glioblastomas observed glomeroid bodies alluding to neoangiogenesis as well as pseudopalisades (hypercellular areas at the periphery of necrotic areas) indicating necrosis and tumor cell migration away from the necrotic, i.e., hypoxic areas within the tumor [36].

Of note, both the maximum CBV and the Cho/Cr and Cho/NAA ratios (individually and in combination) were demonstrated to increase sensitivity and positive predictive value in glioma grading compared to conventional MR imaging [20]. In addition, previous studies reported that PWI [37] and MRSI (increased Cho/Cr ratio) [38] could reduce sampling error by ameliorating the identification of the target areas for biopsy or resection of gliomas. Hence, our findings of inconsistent spatial distributions of the areas of pathologic values of perfusion and spectroscopy favor the suggestion to use fused PWI and MRSI images for a more accurate preoperative brain tumor characterization and selection of stereotactic biopsy targets as well as therapy planning. However, the differentiation between tumor entities (e.g., glioblastoma and lymphoma by means of the voxelwise correlation analysis remains delicate, as significant correlations in all tumor groups and in all value combinations were observed.

A drawback of MRSI with long TE, as used in our study, is that it does not allow the depiction of myo-inositol which has been shown to be a marker for low grade gliomas, i.e., higher in low vs. high grade gliomas [39,40]. The advantage of MRSI over SVS, however, is the better delineation of tumor heterogeneity for which the metabolic characterization and potentially related pathogenesis was the focus of our study. To asses even small malignant foci and to avoid partial volume effects a small voxel size of 1 ml was chosen for MRSI. The drawback is a longer acquisition time or relatively low signal to noise ratio which can cause errors in the peak integrals. However, Stadlbauer et al. showed that high resolution MRSI is capable of providing reliable results [41]. Without more sophisticated offline post processing a correction of these errors and quantitative measurement of the metabolite values was not possible. However, the manufacturer's software offers an approximation of the peak signal intensity integrals and MRSI allows for normalizing the integrals to healthy white matter. Moreover the spectra were thoroughly read, poor quality spectra were excluded and a long TE was used to minimize baseline influence [42]. Additionally, although the histologic types and grades of the tumors are known, the study cannot provide voxel-wise histologic information.

To the authors' knowledge this is the first voxel-wise intra- and interindividual correlational analysis of the MR perfusion parameters CBV and CBF with the MRSI-derived metabolites Cho, Cr, NAA and their metabolite ratios Cho/Cr, Cho/NAA and NAA/Cr in brain tumors complemented by a spatial concordance analysis of the most pathological perfusion and metabolic measures within the brain tumors under investigation.

Our results indicate a significant relationship between vascularization (increased CBV and CBF) and cell proliferation (increased Cr) in II° gliomas and, to a lesser extent, in glioblastomas but not in anaplastic astrocytomas or lymphomas.

Conclusion

In conclusion, our findings suggest that heterogeneity in brain tumors may be due to regional differences in vascularization and metabolism that do not necessarily parallel. The low overall spatial concordance rate of the most pathological perfusion and metabolic alterations within the brain tumors leads us to suggest that the deployment of fused PWI and MRSI imaging would allow a more accurate preoperative brain tumor characterization and selection of stereotactic biopsy targets (and therapy planning) but this warrants future investigation with more detailed, spatial correlation with histology.

Acknowledgement

We thank Dr. Markus Scholz from the Institute for Medical Informatics, Statistics and Epidemiology, Medical Faculty, University of Leipzig, Germany for his support.

The research leading to these results has received funding from the Deutsche Forschungsgemeinschaft (DFG) under Grant Agreement No. SFB 824 ("Imaging for the selection, monitoring and individualization of cancer therapies", Project B6).

Author contributions:

Annette Förschler: Manuscript writing, project development, data collection; Katharina Schwede: Data collection, data analysis; Mirjam Ines Schubert: Manuscript editing; Claus Zimmer: Project development, manuscript editing; Dirk Winkler: Project development

This study was approved by the local ethics committee and has therefore been performed in accordance with the ethical standards laid down in the 1964 Declaration of Helsinki and its later amendments. All patients had given written informed consent prior to their inclusion in the study.

References

1. Paulus W, Peiffer J (1989) Intratumoral histologic heterogeneity of gliomas. A quantitative study. Cancer 64: 442-447.
2. Berlit P, Deuschl G, Elger C, Gold R, Hacke W, et al. (2008) Leitlinien für Diagnostik und Therapie in der Neurologie. Thieme, Stuttgart.
3. Louis DN, Ohgaki H, Wiestler OD, Cavenee WK, Burger PC, et al. (2007) The 2007 WHO classification of tumours of the central nervous system. Acta Neuropathol 114: 97-109.
4. Sugahara T, Korogi Y, Kochi M, Ikushima I, Hirai T, et al. (1998) Correlation of MR imaging-determined cerebral blood volume maps with histologic and angiographic determination of vascularity of gliomas. AJR Am J Roentgenol 171: 1479-1486.
5. Ludemann L, Hamm B, Zimmer C (2000) Pharmacokinetic analysis of glioma compartments with dynamic Gd-DTPA-enhanced magnetic resonance imaging. Magn Reson Imaging 18: 1201-1214.
6. Warmuth C, Gunther M, Zimmer C (2003) Quantification of blood flow in brain tumors: Comparison of arterial spin labeling and dynamic susceptibility-weighted contrast-enhanced MR imaging. Radiology 228: 523-532.
7. Herminghaus S, Pilatus U, Moller-Hartmann W, Raab P, Lanfermann H, et al. (2002) Increased choline levels coincide with enhanced proliferative activity of human neuroepithelial brain tumors. NMR Biomed 15: 385-392.
8. Moffett JR, Ross B, Arun P, Madhavarao CN, Namboodiri AM (2007) N-Acetylaspartate in the CNS: from neurodiagnostics to neurobiology. Prog Neurobiol 81: 89-131.
9. Panigrahy A, Krieger MD, Gonzalez-Gomez I, Liu X, McComb JG, et al. (2006) Quantitative short echo time ^{1}H-MR spectroscopy of untreated pediatric brain tumors: Preoperative diagnosis and characterization. AJNR Am J Neuroradiol 27: 560-572.
10. Hattingen E, Raab P, Franz K, Lanfermann H, Setzer M, et al. (2008) Prognostic value of choline and creatine in who grade II gliomas. Neuroradiology 50: 759-767.
11. Pirzkall A, McGue C, Saraswathy S, Cha S, Liu R, et al. (2009) Tumor regrowth between surgery and initiation of adjuvant therapy in patients with newly diagnosed glioblastoma. Neuro Oncol 11: 842-852.
12. Li X, Lu Y, Pirzkall A, McKnight T, Nelson SJ (2002) Analysis of the spatial characteristics of metabolic abnormalities in newly diagnosed glioma patients. J Magn Reson Imaging 16: 229-237.
13. Hlaihel C, Guilloton L, Guyotat J, Streichenberger N, Honnorat J, et al. (2010) Predictive value of multimodality MRI using conventional, perfusion, and spectroscopy MR in anaplastic transformation of low-grade oligodendrogliomas. J Neurooncol 97: 73-80.
14. Weber MA, Vogt-Schaden M, Bossert O, Giesel FL, Kauczor HU, et al. (2007) MR perfusion and spectroscopic imaging in who grade II astrocytomas. Radiologe 47: 812-818.
15. Wagner M, Nafe R, Jurcoane A, Pilatus U, Franz K, et al. (2011) Heterogeneity in malignant gliomas: A magnetic resonance analysis of spatial distribution of metabolite changes and regional blood volume. J Neurooncol 103: 663-672.
16. Smith JK, Kwock L, Castillo M (2000) Effects of contrast material on single-volume proton MR spectroscopy. AJNR Am J Neuroradiol 21: 1084-1089.
17. Ostergaard L, Weisskoff RM, Chesler DA, Gyldensted C, Rosen BR (1996) High resolution measurement of cerebral blood flow using intravascular tracer bolus passages. Part I: Mathematical approach and statistical analysis. Magn Reson Med 36: 715-725.
18. Rosen BR, Belliveau JW, Vevea JM, Brady TJ (1990) Perfusion imaging with NMR contrast agents. Magn Reson Med 14: 249-265.
19. Hollingworth W, Medina LS, Lenkinski RE, Shibata DK, Bernal B, et al. (2006) A systematic literature review of magnetic resonance spectroscopy for the characterization of brain tumors. AJNR Am J Neuroradiol 27: 1404-1411.
20. Law M, Yang S, Wang H, Babb JS, Johnson G, et al. (2003) Glioma grading: Sensitivity, specificity, and predictive values of perfusion MR imaging and proton MR spectroscopic imaging compared with conventional MR imaging. AJNR Am J Neuroradiol 24: 1989-1998.
21. Rock JP, Scarpace L, Hearshen D, Gutierrez J, Fisher JL, et al. (2004) Associations among magnetic resonance spectroscopy, apparent diffusion coefficients, and image-guided histopathology with special attention to radiation necrosis. Neurosurgery 54: 1111-1119.
22. Bobek-Billewicz B, Stasik-Pres G, Majchrzak H, Zarudzki L (2010) Differentiation between brain tumor recurrence and radiation injury using perfusion, diffusion-weighted imaging and MR spectroscopy. Folia Neuropathol 48: 81-92.
23. Catalaa I, Henry R, Dillon WP, Graves EE, McKnight TR, et al. (2006) Perfusion, diffusion and spectroscopy values in newly diagnosed cerebral gliomas. NMR Biomed 19: 463-475.
24. Toyooka M, Kimura H, Uematsu H, Kawamura Y, Takeuchi H, et al. (2008) Tissue characterization of glioma by proton magnetic resonance spectroscopy and perfusion-weighted magnetic resonance imaging: Glioma grading and histological correlation. Clin imaging 32: 251-258.
25. Batra A, Tripathi RP, Singh AK (2004) Perfusion magnetic resonance imaging and magnetic resonance spectroscopy of cerebral gliomas showing imperceptible contrast enhancement on conventional magnetic resonance imaging. Australas Radiol 48: 324-332.
26. Chang L, McBride D, Miller BL, Cornford M, Booth RA, et al. (1995) Localized *in vivo* ^{1}H magnetic resonance spectroscopy and in vitro analyses of heterogeneous brain tumors. J Neuroimaging 5: 157-163.
27. Galanaud D, Nicoli F, Le Fur Y, Guye M, Ranjeva JP, et al. (2003) Multimodal magnetic resonance imaging of the central nervous system. Biochimie 85: 905-914.

28. Cobbs CS, Whisenhunt TR, Wesemann DR, Harkins LE, Van Meir EG, et al. (2003) Inactivation of wild-type p53 protein function by reactive oxygen and nitrogen species in malignant glioma cells. Cancer Res 63: 8670-8673.
29. Ozturk-Isik E, Pirzkall A, Lamborn KR, Cha S, Chang SM, et al. (2012) Spatial characteristics of newly diagnosed grade 3 glioma assessed by magnetic resonance metabolic and diffusion tensor imaging. Transl Oncol 5: 10-18.
30. Thorsen F, Jirak D, Wang J, Sykova E, Bjerkvig R, et al. (2008) Two distinct tumor phenotypes isolated from glioblastomas show different MRS characteristics. NMR Biomed 21: 830-838.
31. Hartmann M, Heiland S, Harting I, Tronnier VM, Sommer C, et al. (2003) Distinguishing of primary cerebral lymphoma from high-grade glioma with perfusion-weighted magnetic resonance imaging. Neurosci Lett 338: 119-122.
32. Chawla S, Zhang Y, Wang S, Chaudhary S, Chou C, et al. (2010) Proton magnetic resonance spectroscopy in differentiating glioblastomas from primary cerebral lymphomas and brain metastases. J Comput Assist Tomogr 34: 836-841.
33. Ahluwalia MS, Gladson CL (2010) Progress on antiangiogenic therapy for patients with malignant glioma. J Oncol 2010: 689018.
34. Boucher Y, Salehi H, Witwer B, Harsh GR, Jain RK (1997) Interstitial fluid pressure in intracranial tumours in patients and in rodents. Br J Cancer 75: 829-836.
35. Kleihues P, Soylemezoglu F, Schauble B, Scheithauer BW, Burger PC (1995) Histopathology, classification, and grading of gliomas. Glia 15: 211-221.
36. Brat DJ, Castellano-Sanchez AA, Hunter SB, Pecot M, Cohen C, et al. (2004) Pseudopalisades in glioblastoma are hypoxic, express extracellular matrix proteases, and are formed by an actively migrating cell population. Cancer Res 64: 920-927.
37. Maia AC Jr, Malheiros SM, da Rocha AJ, Stavale JN, Guimaraes IF, et al. (2004) Stereotactic biopsy guidance in adults with supratentorial nonenhancing gliomas: Role of perfusion-weighted magnetic resonance imaging. J Neurosurg 101: 970-976.
38. Son BC, Kim MC, Choi BG, Kim EN, Baik HM, et al. (2001) Proton magnetic resonance chemical shift imaging (^{1}H CSI)-directed stereotactic biopsy. Acta Neurochir (Wien) 143: 45-50.
39. Castillo M, Smith JK, Kwock L (2000) Correlation of myo-inositol levels and grading of cerebral astrocytomas. AJNR Am J Neuroradiol 21: 1645-1649.
40. Howe FA, Barton SJ, Cudlip SA, Stubbs M, Saunders DE, et al. (2003) Metabolic profiles of human brain tumors using quantitative *in vivo* ^{1}H magnetic resonance spectroscopy. Magn Reson Med 49: 223-232.
41. Stadlbauer A, Moser E, Gruber S, Buslei R, Nimsky C, et al. (2004) Improved delineation of brain tumors: an automated method for segmentation based on pathologic changes of ^{1}H-MRSI metabolites in gliomas. Neuroimage 23: 454-461.
42. Soher BJ, Young K, Maudsley AA (2001) Representation of strong baseline contributions in ^{1}H MR spectra. Magn Reson Med 45: 966-972.